Defect Chemistry of $La_2Ni_{1-x}M_xO_4$ (M = Mn, Fe, Co, Cu): Relevance to Catalytic Behavior

Mark S. D. Read and M. Saiful Islam*

Department of Chemistry, University of Surrey, Guildford, GU2 5XH, U.K.

Frank King and Fred E. Hancock

I.C.I. Katalco, P.O. Box 1, Billingham, Cleveland, TS23 1LB, U.K.

Received: October 13, 1998

Atomistic computer simulation techniques are used to investigate the defect properties of the $La_2Ni_{1-x}M_xO_4$ (M = Mn, Fe, Co, Cu) layered perovskite which are related to the mode of operation of the catalyst. The theoretical techniques are based upon efficient energy minimization procedures and Mott−Littleton methodology for accurate defect modeling. Effective ionic pairwise interatomic potentials correctly reproduce the tetragonal crystal structure. The formation energy of intrinsic atomic defects of the Schottky and Frenkel type are not particularly favorable. The oxidation of $La_2NiO_{4+\delta}$ was found to be an exothermic process with charge compensation occurring via hole formation preferentially on the Ni site. The highest solubility, for a range of dopants, is calculated for Sr and Ca, in accord with observation. Hole formation was most favorable for Mn > Fe > Co > Ni(undoped) > Cu, demonstrating that Mn and Fe enhance Ni(III) hole formation, which is believed to be an important factor in the observed catalytic activity.

1. Introduction

Complex nickelates such as La_2NiO_4, Nd_2NiO_4, and the $LaNiO_3$ perovskite have received much attention recently, with potential applications in the area of oxidation catalysis.[1−8] Both La_2NiO_4 and Nd_2NiO_4 are nickel analogues of the cuprate high T_C superconductors, and the properties of these oxides may be tailored to specific applications by means of chemical doping. For example, the partial substitution of the La^{3+} site with low-valent cations greatly alters the catalytic and electrical characteristics of the material. This type of "acceptor" doping leads to charge compensation by the stabilization of transition metal ions in higher valence states (e.g. Ni^{3+}) and/or by the formation of oxygen vacancies.

Another potential application relates to the catalytic decomposition of hypochlorite, which is a component of waste effluent within the chlorine industry.[9] Chlorine manufacturers are required to control their emissions to the atmosphere, which is effected by converting gaseous chlorine into the soluble hypochlorite. Despite the useful disinfectant properties of hypochlorite solution, generation by this method is surplus to requirements and hence has to be converted to a less harmful waste product. This is currently achieved via homogeneous catalysis with finely suspended metal hydroxide (usually nickel) which is difficult to separate from the effluent and ends up in the discharge. Hence the net result is that one pollutant has been replaced by another, since nickel, cobalt, and copper are all toxic materials. A fixed bed (heterogeneous) catalytic system would provide an effective solution to this problem.

The investigations concerning the doped La_2NiO_4 catalysts have mainly focused on testing studies of activity behavior.[1−7] It is clear, however, that solid-state properties such as the precise role of structural defects and dopants, as well as the nature of redox reactions leading to the formation of electron−hole centers are not fully characterized and are crucial to the proper understanding of the catalytic properties. During the last decade, computer modeling techniques[10,11] have made widespread contributions to the study of defect, ion transport, and surface properties of a wide variety of oxide compounds, including catalysts[12−15] and superconductors.[16,17] The present simulations of the La_2NiO_4 bulk are an informative preliminary to more complex simulations of the surfaces, which are currently being undertaken. Before discussing the results of our studies, we briefly describe the simulation approach employed.

2. Methodology

The atomistic simulations presented here use the same methodology for the treatment of perfect and defective lattices as employed in our previous studies of solid catalysts (e.g. La_2O_3,[18] CeO_2-ZrO_2,[19] and $LaMO_3$[20]). The methods are based upon the specification of an interatomic potential model which expresses the total energy of the system as a function of the atomic coordinates. For ceramic oxides, the calculations are commonly formulated within a Born model representation, with the total energy partitioned into long-range Coulombic interactions and a short-range analytical function to model overlap repulsions and van der Waals forces of the Buckingham form:

$$\phi_{ij}(r_{ij}) = A_{ij}\exp\left(\frac{-r_{ij}}{\rho_{ij}}\right) - \left(\frac{C_{ij}}{r_{ij}^{6}}\right) \qquad (1)$$

Because charge defects will polarize other ions in the lattice, ionic polarizability must be incorporated into the potential model. The shell model[21] provides a simple mechanistic description of such effects and has proved to be effective in simulating the dielectric and lattice dynamic properties of ceramic oxides. Static simulations of the perfect lattice give the crystal structure and the lattice energy. It should be stressed, as argued previously,[11] that employing such a model does not

* To whom correspondence should be addressed. E-mail: m.islam@surrey.ac.uk.

10.1021/jp984059s CCC: $18.00
Published on Web 02/13/1999

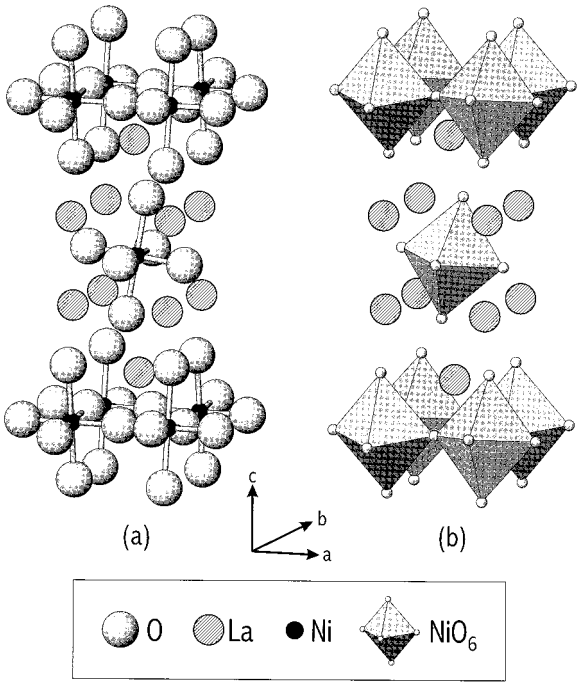

Figure 1. Crystal structure of La_2NiO_4 showing (a) atom positions and (b) nickel−oxygen octahedra.

necessarily mean that the electron distribution corresponds to a fully ionic system and that the general validity of the potential model is assessed primarily by its ability to reproduce observed crystal properties. In practice, it is found that models based on formal charges work well even for some semicovalent compounds such as silicates and zeolites.

An important feature of these calculations is the treatment of lattice relaxation about the point defect or dopant ion. The celebrated Mott−Littleton approach[22] is to partition the crystal lattice into two regions so that ions in a spherical inner region surrounding the defect are relaxed explicitly. In contrast, the remainder of the crystal, where the defect forces are relatively weak, is treated by more approximate quasicontinuum methods. The explicit simulation of the inner region uses efficient energy minimization methods which make use of first and second derivatives of the energy functions with respect to ion coordinates. These perfect and defective lattice methods are embodied in the CASCADE[23] and GULP[24] codes.

The short-range potential parameters assigned to each ion−ion interaction were derived by empirical fitting to the observed structural properties. At low temperature (≤80 K), La_2NiO_4 crystallizes with a tetragonal unit cell (space group $P4_2/ncm$).[25] Isostructural to La_2CuO_4, this structure (shown in Figure 1) is that of a layered perovskite. Integral ionic charges are presumed, i.e. 3+ for La and 2− for O, which enables a simple definition of hole states (as Ni^{3+}) and the useful concept of isovalent or aliovalent dopant substitution. The potential parameters were transferred from recent simulation studies on similar materials; details of the potential and shell model parameters used in this study are given in Table 1. A comparison between calculated and experimental properties, presented in Table 2, shows that differences between the initial and final cell parameters are less than 0.5% and the bond lengths were comparable with the maximum discrepancy being 0.08 Å. This clearly shows that the potentials for La_2NiO_4 correctly reproduce the observed structure, without the need for employing empirical fitting procedures.

TABLE 1: Interatomic Potentials for La_2NiO_4

	short-range parameters			shell model[a]	
interaction	A (eV)	ρ (Å)	C (eV/Å^6)	Y (|e|)	k (eV/Å^2)
		(a) Perfect Lattice			
$La^{3+}\cdots O^{2-}$ [b]	1545.21	0.3590	0.0	−0.250	145.0
$Ni^{2+}\cdots O^{2-}$ [c]	641.20	0.3372	0.0	2.000	99999.0
$O^{2-}\cdots O^{2-}$ [d]	22764.30	0.1490	43.0	−2.389	42.0
		(b) Dopants			
$Mg^{2+}\cdots O^{2-}$ [c]	1428.5	0.2945	0.0	1.585	361.6
$Ca^{2+}\cdots O^{2-}$ [c]	1090.4	0.3437	0.0	3.135	110.2
$Sr^{2+}\cdots O^{2-}$ [c]	959.1	0.3721	0.0	3.251	71.7
$Ba^{2+}\cdots O^{2-}$ [c]	905.7	0.3976	0.0	9.203	459.2
$Mn^{2+}\cdots O^{2-}$ [c]	1007.4	0.3262	0.0	3.420	95.0
$Fe^{2+}\cdots O^{2-}$ [c]	1207.6	0.3084	0.0	2.997	62.9
$Co^{2+}\cdots O^{2-}$ [e]	1491.7	0.2951	0.0	3.503	110.5
$Cu^{2+}\cdots O^{2-}$ [e]	3799.3	0.24273	0.0	2.000	999999.0

[a] Y and k are the shell charge and spring constant, respectively. [b] Reference 31. [c] Reference 32. [d] Reference 17. [e] Reference 33.

TABLE 2: Calculated and Observed Cell Parameters and Interatomic Separations for La_2NiO_4

parameter	$r_{(expt)}$ (Å)[a]	$r_{(calcd)}$ (Å)	|Δ| (Å)
a, b	5.4995	5.5732	0.0737
c	12.5052	12.2676	0.2376
Ni···O1	1.9540	1.9611	0.0070
Ni···O1′	1.9444	1.9434	0.0001
Ni···O2	2.2281	2.3075	0.0790

[a] Experimental values from ref 25.

TABLE 3: Calculated Energies of Isolated Atomic Defects[a]

type of defect	formation energy (eV)
La^{3+} vacancy (V'''_{La})	42.33
Ni^{2+} vacancy (V''_{Ni})	28.34
O^{2-} (1) equatorial vacancy ($V^{\bullet\bullet}_O$)	17.53
O^{2-} (2) equatorial vacancy ($V^{\bullet\bullet}_O$)	17.85
O^{2-} apical vacancy ($V^{\bullet\bullet}_O$)	18.15
La^{3+} interstitial ($La^{\bullet\bullet\bullet}_i$)[b]	−29.89
Ni^{2+} (1) interstitial ($Ni^{\bullet\bullet}_i$)[b]	−20.35
O^{2-} interstitial (O''_i)[b]	−13.50

[a] Region I contains 308 ions. [b] Interstitial site at ($^1/_4$, $^1/_4$, $^1/_4$).

3. Results and Discussion

3.1. Interstitial Oxygen and Oxidation. For superconducting $La_2CuO_{4+\delta}$ the doping mechanism responsible for metallic behavior has been shown to be the inclusion of excess lattice oxygen. Since the solubility for the excess oxygen defect in this system is low, detailed studies of the structure and behavior of the defect have been limited due to difficulties in sample preparation. As an alternative approach to studying the structure and behavior of the excess-oxygen defect, Jorgensen et al.[26] have synthesized and examined samples of the isostructural compound $La_2NiO_{4+\delta}$ which exhibits a wide range of oxygen stoichiometry. Calculations were first performed on the energies of isolated point defects (vacancies and interstitials) which are given in Table 3. In all cases, the lattice ions surrounding the defect are allowed to relax in the energy minimization procedure. The oxygen vacancy energies indicate that it is more favorable to form vacancies in the equatorial rather than in the axial position. When the position of the interstitial oxygen was investigated, the calculations showed that the position in between the LaO and NiO_2 layers, (0.25, 0.25, 0.57), was extremely unfavorable, and the preferred position was predicted to lie between adjacent LaO layers at ($^1/_4$, $^1/_4$, $^1/_4$).

Figure 2 shows that after minimization there is extensive localized restructuring of the crystal lattice. Indeed the four

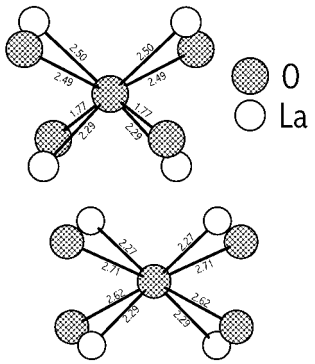

Figure 2. Interatomic distances from the oxygen interstitial to its eight nearest neighbors in $La_2NiO_{4+\delta}$.

TABLE 4: Frenkel and Schottky Energies

type of defect	formation energy (eV/defect)
Frenkel	
La	6.22
Ni	4.00
O	2.33
Schottky	
$[La_2NiO_4\uparrow]$	2.24
Schottky-like	
$[La_2O_3\uparrow]$	1.99
$[NiO\uparrow]$	2.69

neighboring La ions are attracted to the interstitial ion, and the two nearest oxygen ions in the LaO plane above the interstitial are repelled slightly. The largest displacement occurs with the two nearest oxygen ions from the lower LaO plane. The calculated O−O distances between the interstitial and the two oxygen ions from the upper LaO plane have increased by 0.25 Å, and the two oxygen ions from the lower LaO plane by 0.90 Å. The La ions from the upper plane are displaced toward the interstitial by 0.22 Å and those in the lower plane to a lesser extent by 0.06 Å. In summary, the interstitial oxygen has attracted neighboring La ions and displaced the neighboring O ions by average values of 0.14 and 0.58 Å, respectively. These results are in accord with Jorgensen et al.'s[26] observation from neutron powder diffraction studies of $La_2NiO_{4+\delta}$ that the neighboring oxygens to the interstitial defect are displaced by ~0.5 Å from their normal lattice sites. Another study which modeled the structure of La_2NiO_4 by means of bond valences[27] also places the interstitial oxygen between the LaO planes.

The individual point defect energies are then combined to give formation energies for Frenkel and Schottky disorder (reported in Table 4). The Frenkel defects can be represented by the following reactions using Kroger−Vink notation:

$$La_{La}^{\times} \rightleftharpoons V_{La}''' + La_i^{\bullet\bullet\bullet} \quad (2)$$

$$Ni_{Ni}^{\times} \rightleftharpoons V_{Ni}'' + Ni_i^{\bullet\bullet} \quad (3)$$

$$O_O^{\times} \rightleftharpoons V_O^{\bullet\bullet} + O_i'' \quad (4)$$

Similarly, the Schottky defect can be expressed as

$$2La_{La}^{\times} + Ni_{Ni}^{\times} + 4O_O^{\times} \rightleftharpoons 2V_{La}''' + V_{Ni}'' + 4V_O^{\bullet\bullet} + La_2NiO_{4(surf)} \quad (5)$$

From examination of the calculated energies in Table 4, it is evident that the simulations predict that the formation of intrinsic defects is not highly favorable. However the energetically preferred mode of intrinsic defect would be of the La_2O_3 Schottky type involving the creation of La^{3+} and O^{2-} vacancies.

TABLE 5: Hole Formation and Oxidation Energies

type of defect	formation energy (eV/defect)
$h_{Ni}^{\bullet}$	0.30
$h_O^{\bullet}$ (equatorial)	6.79
$E_{oxidation}$	−1.52

It is known that the $La_2NiO_{4+\delta}$ crystal undergoes an oxidation process whereby extra oxygen (δ) is accomodated into the lattice as interstitial ions, with compensation by hole formation.

$$^1/_2O_2 \rightleftharpoons O_i'' + 2h^{\bullet} \quad (6)$$

The formation of a positive hole on both oxygen and nickel sites was examined. Both mechanisms were simulated as a combined process of removing a Ni^{2+}/O^{2-} from a lattice site to infinity, and then introducing a Ni^{3+}/O^{-} ion into the vacant lattice site from infinity. The relevant ionization energies were subsequently used in conjunction with the calculated defect energies to derive the total hole formation energy. Table 5 summarizes these hole formation energies.

By combining defect energies, the energy of oxidation was calculated to be −1.52 eV per hole which is in reasonable quantitative agreement with the experimentally determined value of -1.12 ± 0.15 eV using high-temperature reaction calorimetry.[28] DiCarlo et al.[28] propose that oxidation in the nickelates involves different hole states in comparison to the cuprates, and that these probably occupy predominantly in the Ni 3d-type band, chemically described as "Ni^{3+}" species. These results agree with our predictions that the oxidation process is exothermic to readily produce oxygen interstitials and Ni^{3+} holes in $La_2NiO_{4+\delta}$.

3.2. Dopant Substitution of La_2NiO_4. Experimental studies have shown that the addition of cation dopants to mixed metal oxides is effective in promoting catalysis. The simulation approach is based on assessing the energetics of dissolution of such aliovalent ions and the nature of the charge-compensating defects. The most straightforward mode of dopant incorporation into the host La_2NiO_4 matrix is as a substitutional ion at a La^{3+} site. In this study, alkaline earth metals were first investigated. Since these ions are divalent, on substituting for the trivalent La ion, a charge-compensating mechanism must occur. This can be represented by two defect equations involving either oxygen vacancy or hole (Ni^{3+}) formation:

$$2MO + 2La_{La}^{\times} + O_O^{\times} \rightleftharpoons 2M_{La}' + V_O^{\bullet\bullet} + La_2O_{3(surf)} \quad (7)$$

$$2MO + 2La_{La}^{\times} + {}^1/_2O_2 \rightleftharpoons 2M_{La}' + 2h^{\bullet} + La_2O_{3(surf)} \quad (8)$$

where MO signifies the dopant oxide and M_{La}' the dopant substitutional. The energies of solution were evaluated by combining appropriate defect and cohesive energy terms.

Figure 3 presents the solution energies versus ionic radius for both charge compensation mechanisms. Two main points emerge from these results. First, the most favorable mode of charge compensation is clearly the formation of holes (Ni^{3+}). This is consistent with spectroscopic studies[7,8,29] of the valence band density of states which find that holes are created by Sr doping in La_2NiO_4. It is believed that higher valence Ni is correlated to the activity of these nickelate catalysts, a point to which we return below. Second, the most favorable solution energy, and hence the highest solubility, is predicted for Sr^{2+}, although Ca^{2+} also has a low energy. This accords with

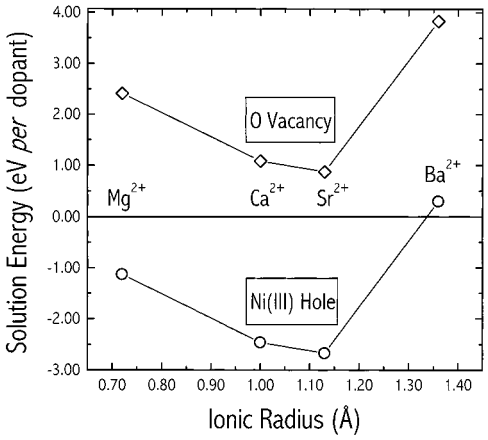

Figure 3. Plot of solution energy as a function of ionic radius for alkaline earth metal dopants in La_2NiO_4.

TABLE 6: Solution Energies for Transition Metal Substitution of Ni^{2+} in La_2NiO_4

dopant species	solution energy (eV)
$Mn_{Ni}^{\times}$	−0.55
$Fe_{Ni}^{\times}$	−0.84
$Co_{Ni}^{\times}$	−0.88
$Cu_{Ni}^{\times}$	−1.67

experimental work in which Sr is the most commonly used acceptor dopant leading to enhanced activity.[5] In addition, we find a degree of correlation between the calculated solution energy and the dopant ion size with minima near the La^{3+} radius (1.06 Å).

In general, these results are consistent with experimental thermochemical measurements[28] in which DiCarlo et al. find that lanthanum nickelates differ in several important respects from the cuprates. First, the oxygen vacancy concentration is small, making the energetic effects of oxygen vacancy ordering far less important. The second important difference is in the oxidation mechanisms. All the nickelates that were studied are in highly oxidized states (at 701 °C, the formal nickel valence is >2.3). Consequently, samples with lower levels of doping ($La_{2-x}A_xNiO_4$, $x \leq 0.1$ (A = Ba, Sr)) have significant concentration of interstitial oxygen. Third, the enthalpy of oxidation in nickelates, unlike cuprates, is not dependent upon whether the substitutional cation was Ba or Sr, suggesting that the nature of hole states is different in the nickelates.

In addition to alkaline earth substitution for La^{3+}, we also considered the substitution of the Ni^{2+} site with divalent transition metal ions, which does not require charge compensation. The reaction scheme for this process is described by the defect equation

$$MO + Ni_{Ni}^{\times} \rightleftharpoons M_{Ni}^{\times} + NiO_{(surf)} \quad (9)$$

The solution energies (Table 6) suggest favorable substitution of Ni by the transition metal dopant. It is evident from Table 6 that the lowest solution energy is for Cu^{2+}, which is consistent with the formation of the isostructural and well-known high T_C superconducting material La_2CuO_4.

3.3. Sr Doping of $La_2Ni_{0.75}M_{0.25}O_4$ (M = Mn, Fe, Co, Cu). It has been shown in experimental studies that codoping La_2NiO_4 with Fe leads to an increase in catalytic activity for hypochlorite decomposition with optimum performance when approximately 25% of the Ni has been replaced.[9] In contrast, the catalytic activity is reduced when codoped with Cu on the

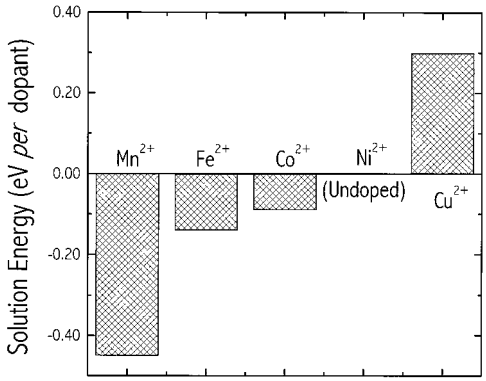

Figure 4. Plot of solution energy for Sr in $La_2Ni_{0.75}M_{0.25}O_4$ (M = Mn, Fe, Co, Cu) systems.

TABLE 7: Hole Formation in $La_2Ni_{0.75}M_{0.25}O_4$ (M = Mn, Fe, Co, Cu)

	hole formation energy (eV)	
M	Ni^{3+}	M^{3+}
Ni (pure La_2NiO_4)	0.30	
Mn	−0.17	3.86
Fe	0.14	3.66
Co	0.19	2.81
Cu	0.62	1.50

Ni site. To investigate these trends, calculations were performed on the La_2NiO_4 system doped with other transition metals (Mn, Fe, Co, Cu), replacing the Ni to levels of 25%.

In a similar manner to the mechanism of Ni^{3+} hole formation, the possibility exists for the divalent transition metal ions to change their formal valence state to form trivalent M^{3+} holes. Calculations examining these various mechanisms are listed in Table 7. It is evident from these results that Ni^{3+} holes are predicted to form more easily in the $La_2Ni_{0.75}M_{0.25}O_4$ systems. Indeed all the M^{3+} holes have significantly larger formation energies than the corresponding Ni^{3+} holes. Table 7 also illustrates that Mn and Fe enhance Ni^{3+} hole formation, whereas this process is less favorable for Cu doping.

Focusing our calculations on Sr as the most soluble dopant, a trend was examined between the Sr solution energies for the $La_2Ni_{0.75}M_{0.25}O_4$ system and is shown in Figure 4. This indicates that the trend related to increased Sr solubility and consequently Ni^{3+} hole formation follows the order

$$Mn > Fe > Co > Ni(undoped) > Cu$$

The results therefore suggest that partial substitution of Mn, Fe, and Co for Ni enhances Ni(III) hole formation, which is believed to be an important factor in the observed catalytic activity of these systems. Indeed, the role of Ni(III) species as active sites in nickelate perovskites is well established in other catalytic studies of, for example, the oxidation of NH_3.[5,30] It is already known that Fe^{2+} incorporation improves the catalytic performance of the oxide[9] whereas Cu doping reduces the activity. However, it should be noted that our calculations (Table 6) have found that Mn^{2+} has the most unfavorable solution energy of these Mn^{2+} dopants, indicating low solubility into La_2NiO_4. Our simulations are consistent with recent photoemission studies of the $La_{2-x}Sr_xNi_{1-y}Fe_yO_{4+\delta}$ system which indicate that the Ni valency increases with Sr doping and that Ni(III) is more easily produced by the presence of Fe doping.[7,8]

Focusing on Fe as the codopant, the extent to which Ni^{3+} holes were stabilized with variation in Fe concentration was also studied. We find that the stabilization of the hole sites is

dependent upon the position of the Fe ion: the formation energy of a Ni^{3+} hole when the Fe ion is situated at the nearest-neighbor position is nearly 0.4 eV lower than when the Fe is at the next-nearest-neighbor position. It is evident from these results that the Ni^{3+} hole is stabilized by the presence of an Fe ion at the nearest-neighbor site, i.e. there is an oxygen bridge between Fe and Ni ions allowing the stabilization transfer. Indeed, King and Hancock[9] postulate that the mechanism of "iron promotion" in $La_{2-x}Sr_xNi_{1-y}Fe_yO_{4+\delta}$ appears to be related to the increase in the Ni(III) ESR signal that is observed and to the possibility of Ni(IV). Furthermore, they observe the system to show strong Fe−O−Ni interactions and propose that the presence of iron facilitates charge transfer between the Ni(II) and Ni(III) ions.

4. Conclusions

The present study has illustrated that, by employing computer simulation techniques, we can investigate dopant substitution and hole formation in La_2NiO_4 that contributes to the understanding of key solid state properties relevant to its catalytic behavior. In particular, the simulations allow us to rationalize, based on quantitative results, why certain dopants enhance the catalytic performance. Our discussion has drawn attention to the following main features:

1. The position of interstitial oxygen ions was found to be most favorable between adjacent LaO layers, in accord with neutron diffraction data from air-oxidized $La_2NiO_{4+\delta}$. The oxidation reaction involving extra oxygen as interstitial ions is predicted to be exothermic in agreement with thermochemical measurements.

2. The formation of intrinsic atomic defects is not favorable, although the energetically preferred mode would be of the La_2O_3 Schottky type.

3. Cation substitution of the La site by alkaline earth metals shows that the most soluble dopant is predicted to be Sr^{2+} and that the most favorable mode of charge compensation is via the formation of Ni^{3+} holes. This is consistent with models in which Ni^{3+} species are correlated to the observed catalytic activity for hypochlorite decomposition.

4. On Sr doping of the solid solutions $La_2Ni_{0.75}M_{0.25}O_4$ (M = Mn, Fe, Co, Cu), it is evident that both Mn and Fe enhances Ni^{3+} hole formation which would promote overall reactivity of the catalyst material. These results accord well with observation in which Fe incorporation improves the catalytic performance whereas Cu doping depresses the activity. It is also found that the Ni^{3+} hole is stabilized by the presence of Fe at the nearest-neighbor position, through strong Fe−O−Ni interactions.

Acknowledgment. This work is supported by a CASE studentship with ICI Katalco (M.S.D.R.). We thank Prof. W. R. Flavell and Dr. J. Gale for helpful discussions. The simulations were performed on the supercomputer facilities at the Rutherford Appleton Laboratory, Oxford, UK.

References and Notes

(1) Tagawa, T.; Imai, H. *J. Chem. Soc., Faraday Trans.* **1998**, *84*, 923.
(2) Ladavos, A. K.; Pomonis, P. J. *Appl. Cata. B* **1993**, 27.
(3) Choisnet, J.; Abadzhieva, N.; Stefanov, P.; Klissurski, D.; Bassat, J. M.; Rives, V.; Minchev, L. *J. Chem. Soc., Faraday Trans.* **1994**, *90*, 1987.
(4) Ling, T. R.; Chen, Z. B.; Lee, M. D. *Catal. Today* **1995**, *26*, 79.
(5) Yu, Z.; Gao, L.; Yuan, S.; Wu, Y. *J. Chem. Soc., Faraday Trans.* **1992**, *88*, 3245.
(6) De La Mora, P.; De Teresa, C.; Vicente, L. *Mater. Res. Soc. Symp. Proc.* **1993**, 331.
(7) Flavell, W. R.; Hollingworth, J.; Howlett, J. F.; Thomas, A. G.; Sarker, M.; Squire, S.; Hashim, Z.; Mian, M.; Wincott, P. L.; Teehan, D.; Downes, S.; Hancock, F. E. *J. Synchrotron Radiat.* **1995**, *2*, 264.
(8) Howlett, J. F.; Flavell, W. R.; Thomas, A. G.; Hollingworth, J.; Warren, S.; Hashim, Z.; Mian, M.; Squire, S.; Aghabozorg, H. R.; Sarker, M. M.; Wincott, P. L.; Teeham, D.; Downes, S.; Law, D. S.; Hancock, F. E. *Faraday Discuss.* **1996**, *105*, 337.
(9) King, F.; Hancock, F. E. *Catal. Today* **1996**, *27*, 203.
(10) Catlow, C. R. A. *Computer-Aided Molecular Design*; Richards, W. G., Ed.; IBC Technical Services: London, 1989; Chapter 21.
(11) Cheetham, A. K.; Day, P. *Solid State Chemistry Techniques*; Clarendon Press: Oxford, UK, 1987; Chapter 7.
(12) Catlow, C. R. A.; Jackson, R. A.; Thomas, J. M. *J. Phys. Chem.* **1990**, *94*, 7889.
(13) Nowak, A. K.; Den Ouden, C. J. J.; Pickett, S. D.; Smit, B.; Cheetham, A. K.; Post, M. F. M.; Thomas, J. M. *J. Phys. Chem.* **1991**, *95*, 848.
(14) Islam, M. S.; Ilett, D. J.; Parker, S. C. *J. Phys. Chem.* **1994**, *98*, 9637.
(15) Oliver, P. M.; Watson, G. W.; Kelsey, E. T.; Parker, S. C. *J. Mater. Chem.* **1997**, *7*, 563.
(16) Winch, L. J.; Islam, M. S. *J. Chem. Soc., Chem. Commun.* **1995**, 1595.
(17) Islam, M. S.; Read, M. S. D.; D'Arco, S. *Faraday Discuss.* **1997**, *106*, 367.
(18) Ilett, D. J.; Islam, M. S. *J. Chem. Soc., Faraday Trans.* **1993**, *89*, 3833.
(19) Balducci, G.; Kašpar, J.; Fornasiero, P.; Graziani, M.; Islam, M. S.; Gale, J. D. *J. Phys. Chem. B* **1998**, *102*, 557.
(20) Islam, M. S.; Cherry, M.; Winch, L. J. *J. Chem. Soc., Faraday Trans.* **1996**, *92*, 479.
(21) Dick, B. G.; Overhauser, A. W. *Phys. Rev.* **1958**, *112*, 90.
(22) Mott, N. F.; Littleton, M. T. *Trans. Faraday Soc.* **1938**, *34*, 485; Special issue: *J. Chem. Soc., Faraday Trans. 2* **1989**, *85*(5), 335−579.
(23) Leslie, M. CASCADE code, Daresbury Laboratory, UK, 1982.
(24) Gale, J. D. GULP code (ver 1.1), Imperial College London, UK, 1993.
(25) Rodríguez-Carvajal, J.; Fernandez-Diaz, M. T.; Martínez, J. L. *J. Phys.: Condens. Matter* **1991**, *3*, 3215.
(26) Jorgensen, J. D.; Dabrowski, B.; Pei, S.; Richards, D. R.; Hinks, D. G. *Phys. Rev. B* **1989**, *40*, 2187.
(27) Brown, I. D. *Z. Kristallogr.* **1992**, *199*, 252.
(28) DiCarlo, J.; Mehta, A.; Banschick, D.; Navrotsky, A. *J. Solid State Chem.* **1993**, *103*, 186.
(29) Tan, Z.; Heald, S. M.; Cheong, S. W.; Cooper, A. S.; Moodenbaugh, A. R. *Phys. Rev. B* **1993**, *47*, 12365.
(30) Ramesh, S.; Manoharan, S. S.; Hegde, M. S.; Patil, K. C. *J. Catal.* **1995**, *157*, 749.
(31) Cherry, M.; Islam, M. S.; Catlow, C. R. A. *J. Solid State Chem.* **1995**, *118*, 125.
(32) Lewis, G. V.; Catlow, C. R. A. *J. Phys. C: Solid State Phys.* **1985**, *18*, 1149.
(33) Baetzold, R. C. *Phys. Rev. B* **1988**, *38*, 11304.